

COHESIVE-CRACK MODELING FOR FIBER-REINFORCED CERAMIC COMPOSITES

Túlio Nogueira Bittencourt

*Laboratório de Mecânica Computacional
Laboratório de Estruturas e Materiais Estruturais
Escola Politécnica da Universidade de São Paulo*

José Luiz Antunes de Oliveira e Sousa

*Faculdade de Construção Civil
Universidade Estadual de Campinas*

Abstract

In this paper the application of the fictitious cohesive crack model for two-dimensional problems is explored. The use of interface elements and the finite element method is considered. A defined crack path approach is employed to simulate the propagation process. The fracture zone propagation is closely associated to the interface constitutive model. An example problem for a fiber-reinforced ceramic is presented to illustrate the simulation procedure. The cohesive crack zone is represented by Evans' model, where fiber bridging and pull-out effects are considered. The concepts reviewed here have been reproduced in a condensed form in an extended abstract presented at the *Joint Conference of Italian Group of Computational Mechanics and Ibero-Latin American Association of Computational Methods in Engineering, AIMETA-CILAMCE*, in Padova, Italy

INTRODUCTION

Different known toughening mechanisms may be activated during crack propagation in ceramic materials [1]: (a) surface energy dissipation, (b) micro cracking, and (c) energy dissipation in the wake of the crack path, such as aggregate interlock and bridging. Depending on the assumption of the most important mechanism(s), different crack models have been proposed [2,3,4,5,6,7,8]. However, there is compelling evidence that the most important toughening mechanism in non-transforming ceramics at ambient temperature is energy dissipation in the crack wake [9,10,11,12,13]. The same can be stated for whisker- and fiber-reinforced ceramics [14,15], and other quasi-brittle material such as concrete, cement-based composites and rocks. In this case, a cohesive crack model (CCM) is usually employed to take into account the softening strain localization phenomenon associated with this dissipation mechanism.

A model, proposed by Hillerborg *et al* [4,5] considers the energy dissipation in the wake of the crack path, while neglecting the other two toughening mechanisms. CCM is the state-of-the-art tool to analyze the fracture behavior of quasi-brittle materials, including concrete, cement-based composites, rocks, ceramics, and ceramic composites.

The applicability of CCM to general mixed-mode conditions has been the focus of recent attention. Throughout the 1980's, Ingraffea *et al* [16,17,18,19,20,21] have employed a strategy of singularity near-cancellation to handle mixed-mode crack propagation, with optional load or crack length control. Crack stability was controlled by iterating on the load or crack length until residual values of stress intensity factors were obtained at the tip of the fictitious crack. Direction of crack propagation was computed using these same residual values. This criterion sometimes failed to predict accurately the critical load to produce crack extension because the singular elements at the crack tip perturbed the stress field in the cohesive zone. Moreover, use of these elements was inconsistent with the assumption of singularity cancellation inherent in the CCM.

Recently, an extension of the fictitious crack model to mixed mode propagation has been proposed by Bocca *et al* [8]. They employed a crack length control scheme with a stress-based crack stability criterion. However, only linear softening behavior is possible in this approach.

METHODS

The principle of virtual work is used as the integral statement of equilibrium in the formulation of the cohesive crack problem:

$$\int_V \boldsymbol{\sigma} \cdot \delta \boldsymbol{\varepsilon} dV = \int_V \mathbf{b} \cdot \delta \mathbf{u} dV + \int_S \mathbf{p} \cdot \delta \mathbf{u} dS \quad (1)$$

where V is the volume of the body, S defines the external surface of the body, $\boldsymbol{\sigma}$ is the stress tensor, $\delta \boldsymbol{\varepsilon}$ is the incremental virtual strain tensor, \mathbf{b} is the body force vector acting per unit volume, $\delta \mathbf{u}$ is the incremental virtual displacement vector, and \mathbf{p} is the vector of applied tractions. Expression (1) is the weak form of the equilibrium equations and is valid for any stress-strain constitutive law.

The cohesive crack model assumes that the process zone can be represented by closing tractions \mathbf{p}_c (Figure 1), acting on both crack faces ($\mathbf{p}_c^+ = -\mathbf{p}_c^-$). At the tip of the process zone, the normal component of \mathbf{p}_c equals the ultimate tensile strength of the material. Noting that $S_{\sigma_c/2} = S_{\sigma_c}^+ = S_{\sigma_c}^-$ (Figure 1), one may rewrite (1) as:

$$\int_V \boldsymbol{\sigma} \cdot \delta \boldsymbol{\varepsilon} dV = \int_V \mathbf{b} \cdot \delta \mathbf{u} dV + \int_{S_{\sigma_e}} \lambda \mathbf{p}_e \cdot \delta \mathbf{u} dS + \int_{S_{\sigma_c/2}} \mathbf{p}_c \cdot (\delta \mathbf{u}^+ - \delta \mathbf{u}^-) dS \quad (2)$$

From (2) it is clear that the problem can be treated by superimposing the effects of the body forces, the applied external loads and the cohesive loads when the body volume behaves elastically. The cohesive problem can be stated as:

- (a) for a given load factor λ , find the process zone size so that the ultimate tensile strength is achieved at the tip of the process zone; or alternatively,
- (b) for a given process zone size, find the load factor λ that would allow the ultimate tensile strength to be achieved at the tip of the process zone.

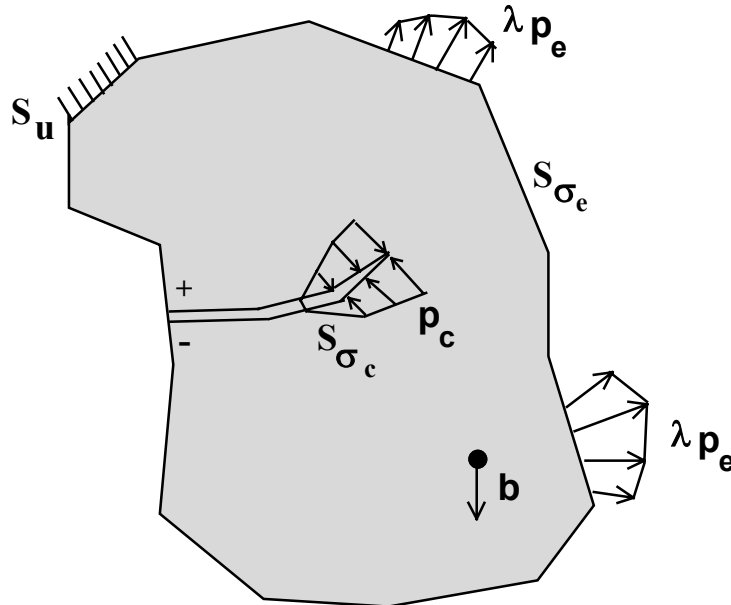


Figure 1 - Cohesive Crack Problem.

Due to the arbitrary nonlinear nature of the softening along S_{σ_c} (Figure 1), a numerical technique is usually employed to solve the cohesive crack problem. A finite element or a boundary element approach is most frequently used to solve the equations of equilibrium. The solution of the fictitious crack problem can be obtained through the use of interface elements placed along a predefined crack path. This scheme is referred here as a defined crack path

strategy [24]. The finite element method is used to generate the solution for each step of propagation. The interface elements are associated to a traction-opening model. Thus, if interface elements are placed along the known crack path, a solution is obtained with the Dynamic Relaxation (DR) solver. The fracture process zone extension is not controlled by the user. It is closely related to the constitutive model of the interface elements. The position of the fictitious crack tip can be estimated from the opening profile. The compressive stiffness (k_c) of the interface model (Figure 2) provides continuity to the constitutive model. This property is crucial for DR. In addition, overlapping of the crack faces may be prevented by introducing a very large value of k_c . The elastic behavior ahead of the fictitious crack tip can be handled for small values of crack opening.

Preferably, loading is defined through applied displacements because an equilibrium search is performed for each value of the load factor. If applied forces are used, the load capacity of the structure should not be exceeded. If it is, equilibrium may be impossible (Figure 3). In this case the solution is computed under force control and only the increasing force path is computed. Alternatively, a displacement control analysis can be used. For this, it is possible to detect snap-back. Unfortunately, points along the snap-back softening path cannot be obtained. A sudden jump in the force for a small displacement increment indicates the presence of a snap-back condition. The force softening with increasing displacements is handled properly through displacement control (see snap-through in Figure 3).

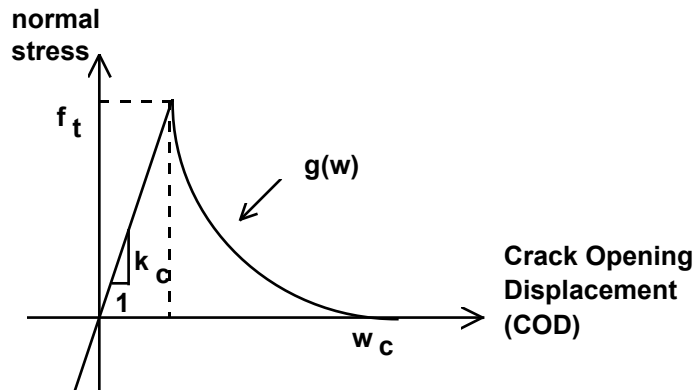


Figure 2 - General softening model of interface elements. The function $g(w)$ is arbitrary.

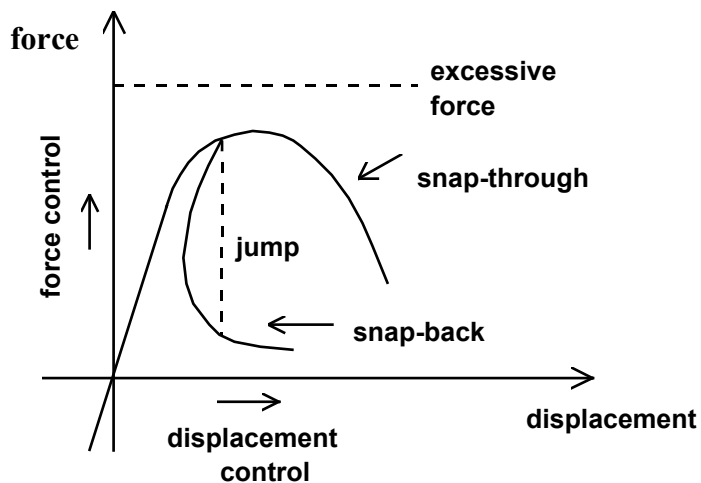


Figure 3 - Possible equilibrium trajectory curves.

RESULTS

The propagation strategy described in the previous section is employed to model the behavior of SEN(B) specimen made of SiC_C(f) composite (Figure 4). The micro-structural parameters influencing the cracking of fiber-reinforced ceramic materials, according to Evans [22,23], are the ratio between interface and matrix fracture toughness, the interface slipping shear stress, the fiber

Weibull parameters (Shape [m] and Scale [S_0]), the matrix specific fracture energy and the volume of fibers (V_f). When the ratio between interface and matrix toughness is less than 0.25, a high fracture toughness for the composite can be achieved due to enhancement of resistance to fiber sliding. Evans assumes the energy consumption in the cracking zone due to matrix cracking and to fiber debonding is negligible when compared to fiber bridging and fiber pull-out effects. This is especially the case when high strength fibers are considered. The stress in a non-broken fiber (σ_b) can be related to the crack opening displacement (w) and to the frictional tangential stress (τ) along the fiber-matrix interface when fiber debonding is neglected [22,23]:

$$\sigma_b = \left[\frac{2\tau E_f (1 + \xi)^{1/2}}{R} \right] w^{1/2} \quad (3)$$

where E_f and R are the elastic modulus and the radius of the fiber, respectively, $\xi = E_f V_f / E_m V_m$, where E_m is the elastic modulus of the matrix and $V_m (= 1 - V_f)$ and V_f are the volume fraction of the matrix and fibers, respectively.

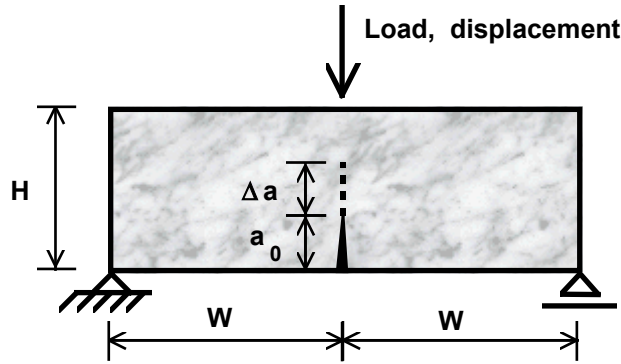


Figure 4 - SEN(B) made of C-SiC ceramic composite. H = 10mm, W = 50mm, Thickness = 5mm.

When the fiber breaks inside the matrix, the pull-out stress across the crack plane is given by:

$$\begin{cases} \sigma_p = \frac{\tau}{R} (h - w) & \text{if } 2h > w \\ \sigma_p = 0 & \text{if } 2h \leq w \end{cases} \quad (4)$$

where h is the distance from the broken fiber to the crack plane. The average stress across the crack plane as a function of the crack opening (w) is given by:

$$\bar{\sigma}(w) = (1 - q)\sigma_b + q\bar{\sigma}_p \quad (5)$$

where q is the percentage of broken fibers at w , and $\bar{\sigma}_p$ is the average pull-out stress computed from (4) for an average value of h .

Fiber failure is often described by weakest link statistics based on the Weibull parameters for shape and scale (m and S_0). Evans employed the concepts described above for negligible residual stress composites and reached at the following expression relating stress to crack opening:

$$\left\{ \begin{array}{l} \sigma = \Sigma V_f \left\{ \left(\frac{w}{\nu} \right)^{1/2} e^{-\alpha} + \frac{1 - e^{-\alpha}}{(1 + \xi)(1 + m)} \left[\Gamma - \frac{\Sigma(1 + m)w}{2E_f \nu} \right] \right\} \quad \text{if } w < w_c \\ \sigma = 0 \quad \text{if } w \geq w_c \end{array} \right. \quad (6)$$

with

$$S_0^m = \frac{2 \pi R^2 \Sigma^{m+1}}{\tau(1 + m)}, \quad \nu = \frac{\Sigma^2 R}{2 E_f (1 + \xi)}, \quad \xi = \frac{E_f V_f}{E_m (1 - V_f)}$$

$$\alpha = \left(\frac{w}{\nu} \right)^{(1+m)/2}, \quad \Gamma = \int_0^{\infty} \beta^{1/1+m} e^{-\beta} d\beta$$

where w_c is the critical crack opening displacement and Σ is the fiber tensile strength, related to m and S_0 . The fracture energy, as long as matrix cracking and fiber debonding are disregarded, is given by:

$$G_F = \int_0^{w_c} \sigma dw \quad (7)$$

The constitutive model described above is employed to model the fracture process in a SEN(B) specimen (Figure 4) made of a SiC_C(f) composite. Experimental results are provided by Gomina *et al.* [25]. The composite was made by the Société Européenne de Propulsion (France) and PAN precursor carbon fibers were employed. The silicon carbide matrix was deposited by the CVD method. A previous numerical study by Llorca [15], from which the model parameters were obtained, is also used for comparison. Llorca employed a simplified crack profile-based method in his computations.

The fiber radius (R) and elastic modulus (E_f) are $3\mu\text{m}$ and 275 GPa . The matrix elastic modulus (E_m) and the volume fraction of fibers (V_f) are 137 GPa and 0.45 . The values of τ , S_0 and m are given as 20 MPa , 121.35 MPa and 2 (Figure 5). A summary of the computed and observed fracture energy and critical crack opening is found in Table 1. The computed values were obtained for the parameters (R , E_f , E_m , V_f , τ , S_0 , m) specified above. The differences between this analysis and Llorca's are probably due to the way the Γ integral in (6) is evaluated. In this analysis, it is computed numerically.

Initial notch lengths, a_0 , of 3.5 mm and 4.1 mm have been considered. A defined crack path analysis under mid-span displacement control (Figure 4) was performed to predict the load-displacement curves (Figure 6 and Figure 7). The loads are computed from the support reactions. As expected, the beam with the larger initial notch is weaker. The present computed results predicted higher maximum loads when compared to the experiments (Table 2). However, a higher fracture energy was employed, for the parameters provided by Llorca [15] and a consistent higher maximum load was obtained. Notice, however, that the computed and observed displacement at peak load (Figures 6 and 7) are close.

Table 1 - Summary of observed and computed results.

Analysis	Fracture Energy (KJ/m ²)	Critical Crack Opening (mm)
Experimental	2.40	not measured
Llorca	3.12	0.43
this analysis	2.98	0.40

Table 2 - Load capacity of the beams.

Analysis	Maximum Load $a_0 = 3.5 \text{ mm (N)}$	Maximum Load $a_0 = 4.1 \text{ mm (N)}$
Experimental	230	185
Llorca	240	200
this analysis	260	220

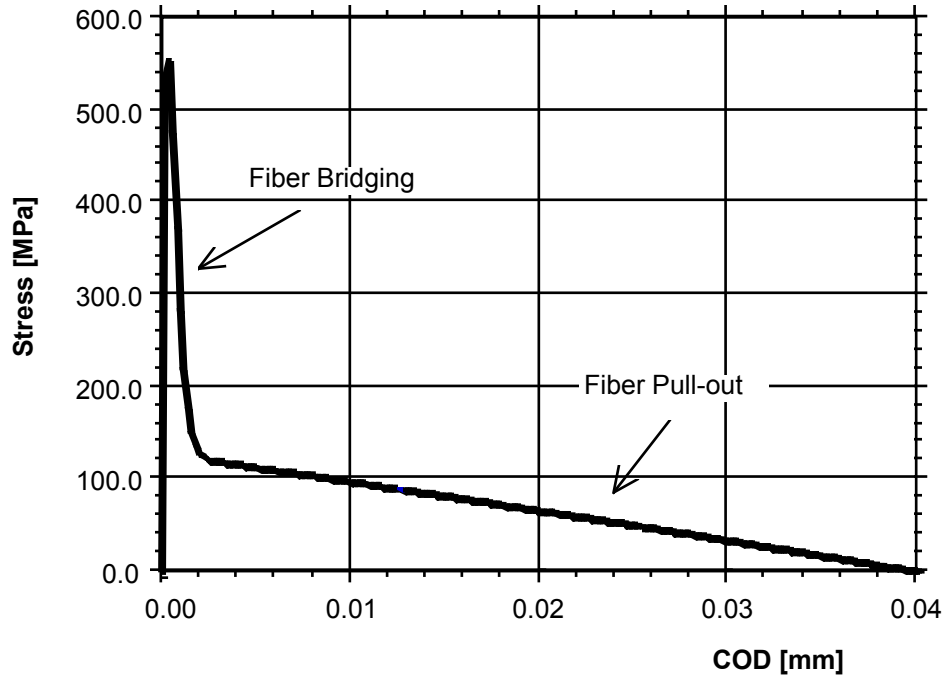


Figure 5 - Stress-crack opening displacement model for SiC_C(f) ceramic composite according to Evans model [22,23].

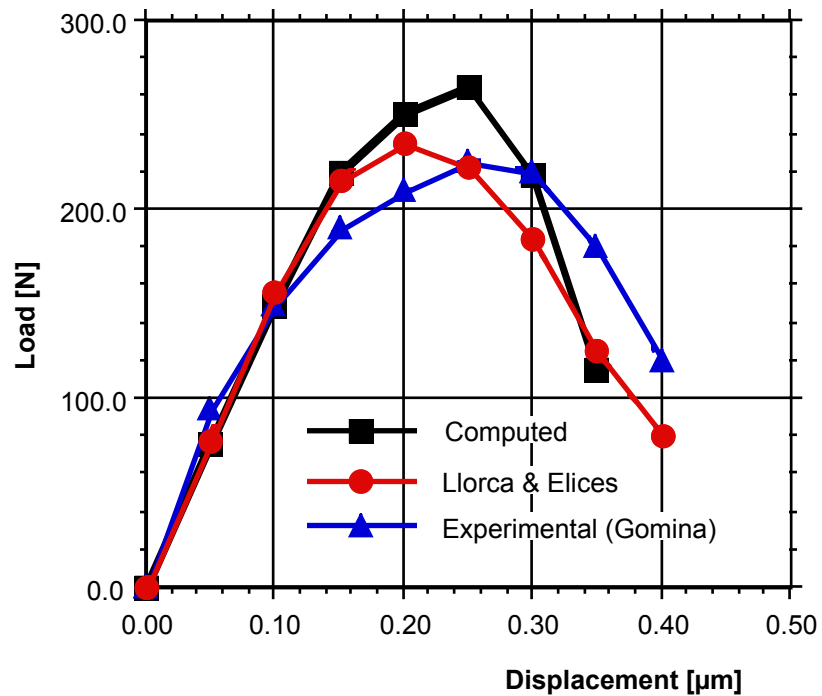


Figure 6 - Load-displacement curve for $a_0 = 3.5 \text{ mm}$.

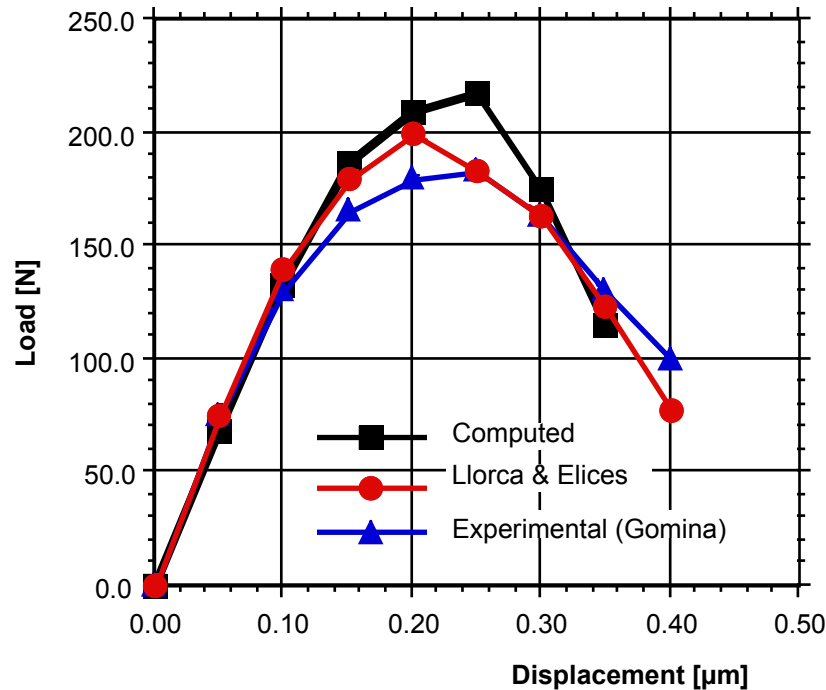


Figure 7 - Load-displacement curve for $a_0 = 4.1$ mm.

CONCLUSION

The application of the fictitious cohesive crack model has been investigated for 2D problems with predefined crack path. Nonlinear interface elements have been used to model the cohesive zone softening behavior.

The application of the mentioned propagation strategy has been applied to model a SEN(B) specimen made of SiC_C(f) composite. Results have shown qualitative agreement. However, the micro-mechanical model has been observed to be very sensitive to the numerical technique to compute its parameters. The differences between this analysis and Llorca's are probably due to this fact. The present computed results predicted higher maximum loads when compared to the experiments. However, it should be noted that a higher fracture energy was employed and a consistent higher maximum load was obtained. It should be pointed out that the computed and observed displacements at peak load are very close.

The example illustrates how the same capabilities used to model the cohesive fracture processes in ceramics can be extended to consider ceramic composite materials. This type of numerical capability can be valuable when designing a new composite material. The influence of each of the composite constituents parameters can be evaluated within the assumptions of a micro-mechanical model. The information can then be processed in order to achieve a higher strength in the presence of initial cracks by enhancing the effective toughness of the ceramic composite.

REFERENCES

1. Shah, S.P., "Whither fracture mechanics for concrete," Keynote Lecture, *Fracture of Concrete and Rock: Recent Developments*, Edited by S.P.Shah, S.E.Swartz, and B.Barr, Elsevier Science Publishers LTD, (1989), pp.1-4.
2. Saouma, V.E., Ingraffea, A.R. and Catalano, D.M., "Fracture toughness of concrete: K_{Ic} revisited," *Journal of Engineering Mechanics Division*, ASCE, Vol.108, N° EM6, (1982), pp.1152-1166.
3. Bazant, Z.P. and Oh, B., "Crack band theory for fracture of concrete," *Materials and Structures*, Vol.16, N° 93, (1983), pp.155-177.
4. Hillerborg, A., Modeer, M., and Petersson, P-E., "Analysis of crack formation and crack growth in concrete by means of fracture mechanics and finite elements," *Cement and Concrete Research*, Vol.6, (1976), pp.773-782.

5. Petersson, P-E., "Crack growth and development of fracture zones in plain concrete and similar materials," *Report TVBM-1006/1-174*, Division of Building Materials, Lund Institute of Technology, Lund, Sweden, (1981).
6. Carpinteri, A., "Interpretation of the Griffith instability as a bifurcation on the global equilibrium," *Application of Fracture Mechanics to Cementitious Composites*, NATO-ARW, (1984), pp.287-316.
7. Jenq, Y. and Shah, S.P, "Two parameter fracture model for concrete," *ASCE, EMD*, Vol.11, N° 10, (1985).
8. Bocca, P., Carpinteri, A. and Valente, S., "Mixed mode fracture of concrete," *International Journal of Solids and Structures*, Vol.27, N° 9, (1991), pp.1139-1153.
9. Swanson, P.L., Fairbanks, C.J, Lawn, B.R, Mai, Y.W., and Jockey, B.J., "Crack interface grain bridging as a fracture resistance mechanism in ceramics: experimental study on alumina," *Journal of American Ceramic Society*, Vol. 70[4], (1987), pp.279-289.
10. Vekinis, G., Ashby, M.F. and Beaumont, P.W.R., "R-curve behaviour of Al₂O₃ ceramics," *Acta Metallurgica*, Vol. 38[6], (1990), pp.1151-1162.
11. Rödel, J., Kelly, J.F. and Lawn, B.R., "In situ measurements of bridged crack interfaces in the scanning electron microscope," *Journal of American Ceramic Society*, Vol. 73[11], (1990), pp.3313-3318.
12. Llorca, J. and Steinbrech, R.W., "Fracture of alumina: an experimental and numerical study," *Journal of Material Science*, Vol. 6, (1991), pp. 383-390.
13. Mai, Y.M., "Fracture and fatigue of non-transformable ceramics: the role of crack-interface bridging," *Fracture Processes in Concrete, Rock and Ceramics*, Edited by Van Mier, J.G.M., London, (1991).
14. Becher, P.F., Hsueh, H., Angelini, P. and Tiegs, T.N., "Toughening behavior in whisker-reinforced ceramic matrix composites," *Journal of American Ceramic Society*, Vol. 71[12], (1988), pp.1050-1061.
15. Llorca, J. and Elices, M., "Fracture resistance of fiber-reinforced ceramic matrix composites," *Acta Metallurgica*, Vol. 38[12], (1990), pp.2485-2492.
16. Ingraffea, A.R. and Gerstle, W.H., "Non-linear fracture models for discrete cack propagation," *Application of Fracture Mechanics to Cementitious Composites*, NATO-ARW, September 4-7, (1984), pp.171-207.
17. Ingraffea, A.R., Gerstle, W.H., Gergely, P. and Saouma, V., "Fracture mechanics of bond in reinforced concrete," *Journal of Structural Engineering*, ASCE, Vol.110, N° 4, (1984), pp.871-889.
18. Hellier, A.K., Sansalone, M., Carino, N.J., Stone, W.C. and Ingraffea, A.R., "Finite-element analysis of the pullout test using a nonlinear discrete cracking approach," *Cement, Concrete, and Aggregates*, Vol.9, N° 1, (1987), pp. 20-29.
19. Swenson, D.V., Ingraffea, A.R., "The collapse of the schoharie creek bridge: A case study in concrete fracture mechanics," *Int. Journal of Fracture*, Vol. 51, (1991), pp.73-92.
20. Wawrzynek, P.A., Boone, T., and Ingraffea, A.R., "Efficient techniques for modeling the fracture process zone in rock and concrete," *Proc. of the Fourth International Conference on Numerical Methods in Fracture Mechanics*, March 23-27, (1987), San Antonio, Texas, A.R. Luxmoore, D.R.J. Owen, Y.S. Rajapakse, and M.F. Kanninen, Editors, pp. 473 - 482.
21. Ingraffea, A.R., "Theory of Crack Initiation and Propagation in Rock," Chapter 3 in *Rock Fracture Mechanics*, B. Atkinson, editor, Academic Press Inc., (1987).
22. Evans, A.G. and Thouless, M.D., "Effects of pull-out on the mechanical properties of ceramic-matrix composites," *Acta Metallurgica*, vol.36, n°3, (1988), pp. 517-522.
23. Evans, A.G., "The mechanical performance of fiber-reinforced ceramic matrix composites," *Materials Science and Engineering*, A107, (1989), pp. 227-239.
24. Bittencourt, T.N., "Computer Simulation of Linear and Nonlinear Crack Propagation in Cementitious Materials," Ph.D. Thesis, Cornell University, (1993).
25. Gomina, M., Themines, D., Chermant, J.L., and Ostertock, F., "An Energy Evaluation for C/SiC Composite Materials," *Int. Journal of Fracture*, vol.34, (1987), pp.219-228.

Address for correspondence:

Túlio Nogueira Bittencourt, Departamento de Engenharia de Estruturas e Fundações, Escola Politécnica da Universidade de São Paulo, Caixa Postal: 61548, CEP:05424-970, São Paulo, Brasil, Email: tbitten@usp.br